BIOCHEMISTRY
including biophysical chemistry & molecular biology

Article

pubs.acs.org/biochemistry

Human tNASP Promotes in Vitro Nucleosome Assembly with Histone H3.3

Daiki Kato, Akihisa Osakabe, Hiroaki Tachiwana, Hiroki Tanaka, and Hitoshi Kurumizaka*

Laboratory of Structural Biology, Graduate School of Advanced Science and Engineering, Waseda University, 2-2 Wakamatsu-cho, Shinjuku-ku, Tokyo, 162-8480, Japan

Supporting Information

ABSTRACT: Nuclear autoantigenic sperm proteins (NASPs) are members of the acidic histone chaperones, which promote nucleosome assembly. In humans, two splicing variants proposed for the somatic and testicular isoforms, sNASP and tNASP, respectively, have been found, and the shorter form, sNASP, reportedly promotes nucleosome assembly with the histone H3 isoforms, H3.1, H3.2, and H3.3. However, the biochemical properties of the longer form, tNASP, have not been reported. tNASP is considered to exist specifically in the testis. Our present results revealed that the tNASP protein is ubiquitously produced in various human tissues, in addition to testis. Unexpectedly, we found that the nucleosome assembly activity of purified tNASP was extremely low with the canonical histone H3.1 or H3.2, but was substantially detected with the replacement histone H3.3 variant. A mutational analysis revealed that the H3.3 Ile89 residue, corresponding to the H3.1 Val89 residue, is responsible for the tNASP-mediated nucleosome assembly with H3.3. A histone deposition assay showed that the H3.3−H4 complex is more efficiently deposited onto DNA by tNASP than the H3.1−H4 complex. These results provide evidence that tNASP is ubiquitously produced in various types of human tissues and promotes in vitro nucleosome assembly with H3 variant specificity.

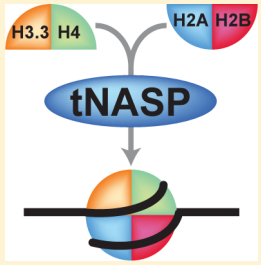

Histones are the protein components of the nucleosome, which is the basic repeating unit of chromatin.[1] In the nucleosome, a 146 base-pair DNA is wrapped around a histone octamer, comprising two H2A−H2B dimers and one H3−H4 tetramer.[2] In the nucleosome assembly process, an H3−H4 tetramer is first deposited onto DNA and forms the H3−H4 tetrasome, in which the DNA is wrapped around an H3−H4 tetramer.[1] Two H2A−H2B dimers are then incorporated into the H3−H4 tetrasome, and the mature nucleosome is formed.[3] These stepwise nucleosome assembly processes are mediated by the histone chaperones.[4−7]

The histone chaperones are acidic proteins that specifically or preferentially promote nucleosome assembly with certain histone isoforms, called histone variants.[8−11] Eight human histone H3 isoforms have been found, as nonallelic isoforms.[12,13] Among the human H3 isoforms, substantial amounts of H3.1, H3.2, and H3.3 are ubiquitously produced in human cells.[14,15] H3.1 and H3.2 are produced during the S-phase of the cell cycle and are incorporated into chromatin by the histone chaperone CAF-1.[16−19] On the other hand, H3.3 is constantly present and is used as a replacement histone H3 that is incorporated into chromatin by the histone chaperone HIRA during and/or after transcription processes.[19,20] H3.3 is also specifically recruited to specific chromosomal loci, such as centromeres and telomeres, by the histone chaperone DAXX.[21−23] In addition, the centromere-specific histone H3 isoform CENP-A (also named cenH3) strictly requires its specific histone chaperone HJURP for centromere targeting.[24,25] In contrast, Nap1, Nap2, and nuclear autoantigenic sperm proteins (NASPs) may be universal histone chaperones, which exhibit low stringency for the histone H3 isoforms during nucleosome assembly, except for the testis-specific H3 variant, H3T.[26,27] Nap1 and NASPs may also function as chaperones for the linker histone H1 and regulate higher order chromatin assembly and disassembly.[28−31] NASPs have been identified as the homologues of *Xenopus laevis* N1/N2, based on their sequence similarities.[32] The N1/N2 protein is an H3−H4 binding protein and may function in the storage and assembly of H3−H4.[33−35] In *Saccharomyces cerevisiae*, the NASP homologue, Hif1, was identified as a protein that specifically interacts with H3−H4 and promotes nucleosome assembly.[36,37] In *Schizosaccharomyces pombe*, Sim3 was reported as a NASP homologue, which may function to promote nucleosome assembly with the centromere-specific H3 variant Cnp1.[38] The histone storage and nucleosome assembly activities are also conserved in the mammalian NASPs.[27,39−41] Therefore, the NASP family proteins are widely conserved in eukaryotes.

Mice lacking the *NASP* gene exhibit embryonic lethality, revealing that it is essential for embryonic development.[42] Interestingly, two types of NASP proteins, shorter and longer forms, are produced from the single *NASP* gene in humans, as splicing variants. The shorter form is named the somatic NASP (sNASP) and is ubiquitously produced in cells.[43] The longer form is named the testicular NASP (tNASP) because its expression was originally found in testis.[43] Purified human sNASP efficiently promotes nucleosome assembly with the

Received: October 18, 2014
Revised: January 10, 2015
Published: January 23, 2015

DOI: 10.1021/bi501307g
Biochemistry 2015, 54, 1171−1179

conventional H3.1, H3.2, and H3.3 histones.[27] However, the biochemical activity of tNASP has not been characterized.

In the present study, we found that the endogenous tNASP protein is ubiquitously produced in various human tissues. We then purified human tNASP as a recombinant protein and discovered that tNASP catalyzed in vitro nucleosome assembly with the H3.3 histone, but its activity was very low with the canonical H3.1 and H3.2 histones. We found that the H3.3-specific Ile89 residue was required for the tNASP-mediated nucleosome assembly. These results suggested that tNASP is functionally distinct from sNASP and may play a specific role in the nucleosome assembly with H3.3, but not the canonical H3.1 and H3.2.

EXPERIMENTAL PROCEDURES

Purification of Recombinant Human NASPs. Human tNASP was produced in *Escherichia coli* cells, as a recombinant protein with an N-terminal hexahistidine (His_6) tag. The DNA fragment encoding tNASP was inserted between the *Nde*I and *Bam*HI sites of the pET15b vector (Novagen), in which the His_6 tag is fused to the N-terminus of tNASP with the thrombin protease recognition site (GE Healthcare). *E. coli* BL21(DE3) cells with an expression vector for the minor tRNAs (Codon(+)RIL; Stratagene) were used as the host strain, and the cells containing the tNASP expression vector were grown on LB plates containing ampicillin (100 μg/mL) and chloramphenicol (35 μg/mL) at 37 °C for 16 h. After incubation, the colonies on the LB plates were collected, inoculated in LB medium containing ampicillin (100 μg/mL) and chloramphenicol (35 μg/mL), and cultured at 30 °C. tNASP was produced by the addition of 0.5 mM isopropyl β-D-thiogalactopyranoside (IPTG), when the cell density reached an OD_{600} = 0.5. After the addition of IPTG, the cells were further cultured at 18 °C for 12 h. The cells producing tNASP were then harvested and disrupted by sonication in 50 mM Tris-HCl (pH 7.5) buffer, containing 500 mM NaCl, 10% glycerol, and 2 mM 2-mercaptoethanol. The cell debris was removed by centrifugation (27216*g*; 20 min), and the resulting cell lysate was mixed with nickel-nitrilotriacetic acid (Ni-NTA) agarose resin (Qiagen) at 4 °C for 1 h, with gentle rotation. The beads were then packed into an Econo-column (Bio-Rad) and washed with 50 mM Tris-HCl (pH 7.5) buffer, containing 10% glycerol, 500 mM NaCl, 2 mM 2-mercaptoethanol, and 5 mM imidazole. His_6-tagged tNASP was eluted by a linear gradient of 5 mM to 500 mM imidazole. The His_6-tag portion was removed from tNASP by a treatment with thrombin protease (5 units/mg of protein), during dialysis against 20 mM Tris-HCl (pH 7.5) buffer, containing 100 mM NaCl, 10% glycerol, 1 mM EDTA, and 2 mM 2-mercaptoethanol. After the removal of the His_6-tag portion, tNASP was subjected to MonoQ (GE Healthcare) chromatography and was eluted by a linear gradient of 100 mM to 400 mM NaCl. The eluted tNASP fraction was further purified by Superdex200 (GE Healthcare) chromatography with 20 mM Tris-HCl (pH 7.5) buffer, containing 100 mM NaCl, 10% glycerol, 1 mM EDTA, and 2 mM 2-mercaptoethanol. tNASP was further purified by MonoQ chromatography and was eluted with a linear gradient of 200 mM to 800 mM NaCl. The purified tNASP fraction was dialyzed against 20 mM Tris-HCl (pH 7.5) buffer, containing 150 mM NaCl, 10% glycerol, 0.1 mM PMSF, 0.5 mM EDTA, and 1 mM dithiothreitol (DTT). sNASP was purified by the same method described previously.[27]

Purification of Recombinant Human Histones. Human histones H2A, H2B, H4, and H3 variants (H3.1, H3.2, H3.3, and H3T) were prepared by the methods described previously.[15,44−46] Briefly, histones were produced in *E. coli* cells as N-terminal His_6-tagged proteins, purified by chromatography on Ni-NTA agarose and MonoS columns (GE Healthcare), treated with thrombin to remove the His_6-tag portion, and freeze-dried. The H2A−H2B and H3−H4 complexes were reconstituted and purified by Superdex200 chromatography, in buffer containing 20 mM Tris-HCl (pH 7.5), 100 mM NaCl, 1 mM EDTA, 1 mM PMSF, 5% glycerol, and 5 mM 2-mercaptoethanol, as described previously.[47]

Western Blotting Analysis of tNASP Produced in Human Tissues. The INSTA-Blot (IMGENEX) membrane was blocked by Blocking One-P (Nacalai Tesque) and washed with TBS-T (20 mM Tris-HCl (pH 7.5), 137 mM NaCl, and 0.1% Tween 20). The membrane was incubated at room temperature with an anti-NASP rabbit polyclonal antibody (1:1000) or an anti-α-tubulin mouse monoclonal antibody (1:5000; Sigma-Aldrich) in solution 1 (TOYOBO), followed by three washes with TBS-T. sNASP was used as the antigen for the production of the anti-NASP antibody, and the resulting anti-NASP polyclonal antibody was confirmed to detect tNASP with recombinant tNASP (Figure 1C). The membrane was further incubated at room temperature with horseradish peroxidase conjugated anti-rabbit IgG (1:1000; GE Healthcare) for NASP or mouse IgG (1:1000; GE Healthcare) for α-tubulin in solution 2 (TOYOBO), followed by three washes with TBS-T. Protein signals were developed by ECL Prime Western Blotting Detection Reagents (GE Healthcare) and detected using an LAS-4000 image analyzer (GE Healthcare).

siRNA Transfection. The NASP-specific Stealth RNAi siRNA (HSS106960, 5′-GGAAUGUAGCUGAACUGGCUCUGAA-3′; Invitrogen) and the control siRNA (Negative Control Hi GC, #462000; Invitrogen) were introduced into HeLa cells by the jetPRIME reagent (Polyplus Transfection). At 3 days after the siRNA transfection, total cellular proteins were fractionated by 12% SDS-PAGE and were immunoblotted with an anti-NASP rabbit polyclonal antibody (1:1000) or an anti-α-tubulin mouse monoclonal antibody (1:5000; Sigma-Aldrich) in solution 1 (TOYOBO).

Supercoiling Assay for Nucleosome Assembly. The supercoiling assay was performed according to the method described previously,[27,47] with modifications. Negatively supercoiled DNA (ϕX174 DNA; New England BioLabs) was relaxed by 1.67 units of wheat germ topoisomerase I (Promega) per 100 ng of DNA, at 37 °C for 150 min. The indicated amounts of tNASP or sNASP were preincubated with H2A−H2B (0.4 μM) and H3−H4 (0.4 μM), at 37 °C for 15 min. Relaxed DNA (100 ng) was then added to the reaction mixture including the NASP−histone complex, in 10 μL of 10 mM Tris-HCl (pH 7.5) buffer, containing 140 mM NaCl, 5 mM DTT, and 2.2 mM $MgCl_2$, which was incubated at 37 °C for 60 min. Reactions were stopped by adding stop solution, containing 20 mM Tris-HCl (pH 8.0), 20 mM EDTA, 0.25% SDS, and 0.5 mg/mL proteinase K (Roche), and the mixtures were further incubated at 37 °C for 15 min. The DNA was then extracted with phenol-chloroform and was analyzed by 1% agarose gel electrophoresis in 1× TAE (40 mM Tris acetate and 1 mM EDTA) with SYBR Gold staining (Invitrogen).

Gel Electrophoretic Mobility Shift Assay for Histone-NASP Binding. tNASP (3 μM) was mixed with the indicated amounts of histone complexes, in 20 mM Tris-HCl (pH 8.0)

DOI: 10.1021/bi501307g
Biochemistry 2015, 54, 1171−1179

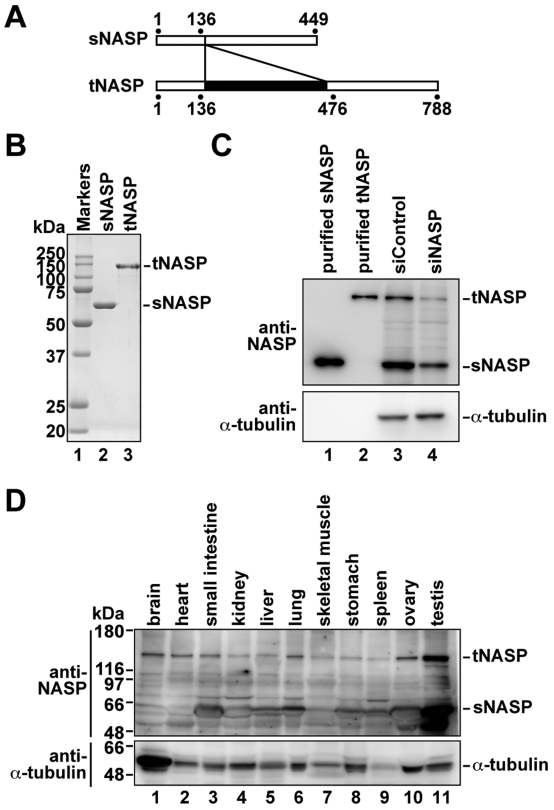

Figure 1. tNASP production in human tissues and tNASP purification. (A) Schematic representations of sNASP and tNASP. (B) Purified sNASP and tNASP. Lanes indicate molecular mass markers (lane 1), sNASP (lane 2), and tNASP (lane 3). (C) Western blotting analysis of sNASP and tNASP from extracts of HeLa cells treated with siRNAs. Lanes 1 and 2 indicate recombinant NASPs, sNASP (lane 1), and tNASP (lane 2). Lanes 3 and 4 indicate total cellular proteins treated with a control siRNA (50 nM) and a NASP-specific siRNA (50 nM), respectively. The lower panel represents the Western blotting analysis of α-tubulin for loading controls. Full images are presented in Supplementary Figure 1, Supporting Information. (D) Western blotting analysis of tNASP and sNASP (upper panel) or α-tubulin (lower panel) in human tissues. The INSTA-Blot (IMGENEX) membrane, blotted with proteins extracted from human tissues, was purchased and used for the analysis. Full images are presented in Supplementary Figure 1.

buffer, containing 100 mM NaCl and 1 mM DTT, and the reaction mixtures were incubated at 25 °C for 60 min. After incubation, the NASP–histone complexes were separated by 5% nondenaturing PAGE in 1× TBE buffer (90 mM Tris base, 90 mM boric acid, and 2 mM EDTA), and the bands were visualized by Coomassie Brilliant Blue staining.

Purification of the tNASP–H3.1–H4 Complex. The tNASP–H3.1–H4 complexes were purified with a Prep Cell apparatus (Bio-Rad) by nondenaturing polyacrylamide gel electrophoresis. The purified tNASP–H3.1–H4 complexes were then analyzed by 16% SDS-PAGE with Coomassie Brilliant Blue staining.

Histone Deposition Assay. tNASP (6 μM) was mixed with the H3.1–H4 or H3.3–H4 complex (6 μM) in 5 μL of 20 mM Tris-HCl (pH 7.5) buffer, containing 110 mM NaCl and 1 mM DTT, at 25 °C for 20 min. sNASP (6 μM) was mixed with the H3.1–H4 or H3.3–H4 complex (10 μM) in 5 μL of 20 mM Tris-HCl (pH 7.5) buffer, containing 110 mM NaCl and 1 mM DTT, at 25 °C for 20 min. After incubation, the samples were then mixed with the indicated amounts of supercoiled DNA in 10 μL of 20 mM Tris-HCl (pH 7.5) buffer, containing 100 mM NaCl and 1 mM DTT, and were further incubated at 25 °C for 60 min. The complexes were then separated by 5% nondenaturing native polyacrylamide gel electrophoresis in 1× TBE buffer, and the bands were visualized by Coomassie Brilliant Blue staining. Band intensities were quantitated by an LAS4000 image analyzer (GE Healthcare). Histone deposition activities were evaluated by the decreasing band intensity of the tNASP–H3–H4 complexes or the increasing band intensity of the free sNASP.

RESULTS

Human tNASP Is Ubiquitously Produced in Human Tissues. Since tNASP was originally found in the testis and embryonic tissues, it was named testicular NASP.[43] Human tNASP is a splicing variant of sNASP, with a 339 amino acid segment inserted just after position 136 of sNASP (Figure 1A). We purified the recombinant human tNASP and sNASP proteins (Figure 1B). The molecular mass of human tNASP is 85 kDa; however, its migration on an SDS-polyacrylamide gel was markedly slower than the expected migration distance, because of its extreme acidity (pI = 4.26). We confirmed that the molecular mass of the purified tNASP protein was about 85 kDa by mass spectrometry (data not shown). These results indicated that human tNASP was correctly produced as the recombinant protein and was purified to near homogeneity.

We then assessed the endogenous tNASP production in human tissues, with an anti-NASP polyclonal antibody. In the HeLa cell extract, this anti-NASP antibody specifically detected the bands migrating at the same distances as recombinant tNASP and sNASP (Figure 1C, lanes 1–3). We knocked down tNASP and sNASP in HeLa cells, using small inhibitory RNA (siRNA), and found that the intensities of these bands were substantially decreased with the NASP-specific siRNA, but not with a control siRNA (Figure 1C, lanes 3 and 4). These results validated the appropriateness of the antibody for evaluating the tissue-specific production of NASPs.

We then used an INSTA-Blot (IMGENEX), in which the proteins extracted from brain, heart, small intestine, kidney, liver, lung, skeletal muscle, stomach, spleen, ovary, and testis were blotted onto a PVDF membrane. Robust production (above the saturation level) of sNASP was detected in all tissues present on this INSTA-Blot membrane (Figure 1D). As expected, tNASP was detected in the testis extract (Figure 1D). However, we also found that substantial amounts of tNASP were ubiquitously produced in other human tissues (Figure 1D).

Human tNASP Preferentially Promotes Nucleosome Assembly with Histone H3.3. Since tNASP belongs to the acidic histone chaperone family, we tested its nucleosome assembly activity. To do so, we used a supercoiling assay (Figure 2A). In this assay, tNASP was incubated with relaxed circular DNA, in the presence of the human histone H2A–H2B and H3–H4 complexes (Figure 2B). Negative supercoils would be introduced into the DNA if the nucleosomes were properly assembled on the DNA by the tNASP activity.

We then performed the supercoiling assay with various histone H3 isoforms, including H3.1, H3.2, H3.3, or H3T (Figure 2B). As reported previously,[27] sNASP efficiently promoted the nucleosome assembly with the canonical histone isoforms, H3.1 and H3.2, and the major replacement histone H3 variant, H3.3 (Figure 2C). Surprisingly, we found that

DOI: 10.1021/bi501307g
Biochemistry 2015, 54, 1171–1179

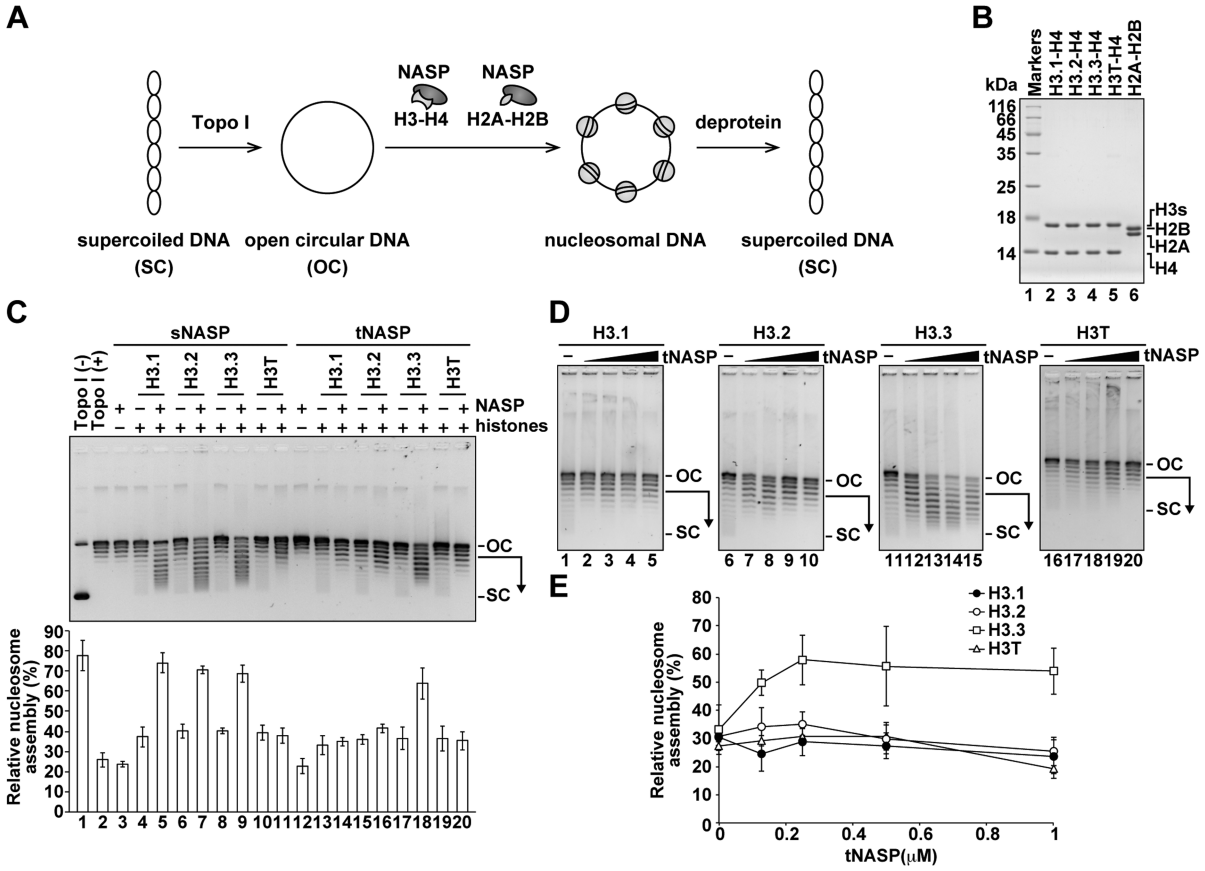

Figure 2. Nucleosome assembly activity of tNASP. (A) Schematic representation of the supercoiling assay. Reactions were conducted in the presence of topoisomerase I (Topo I). (B) Purified H3 variants complexed with H4. Lanes indicate molecular mass markers (lane 1), H3.1−H4 (lane 2), H3.2−H4 (lane 3), H3.3−H4 (lane 4), H3T−H4 (lane 5), and H2A−H2B (lane 6). (C) Nucleosome assembly activities of sNASP and tNASP, assessed by a supercoiling assay. Relaxed DNA (lane 2) was incubated with histones (0.4 μM) in the absence (lanes 4, 6, 8, 10, 13, 15, 17, and 19) or presence (lanes 5, 7, 9, 11, 14, 16, 18, and 20) of sNASP or tNASP (1 μM). The nucleosome assembly reactions were conducted with H3.1−H4 (lanes 4, 5, 13, and 14), H3.2−H4 (lanes 6, 7, 15, and 16), H3.3−H4 (lanes 8, 9, 17, and 18), or H3T−H4 (lanes 10, 11, 19, and 20) in the presence of H2A−H2B (0.4 μM). Lane 1 indicates the supercoiled DNA, and lanes 3 and 12 indicate the negative control experiments without histones, in the presence of sNASP (1 μM) and tNASP (1 μM), respectively. The bar graphs under the gel images represent the nucleosome-assembly activities of NASPs. The supercoiled DNA bands generated by the NASP-mediated nucleosome assembly are indicated by the arrow, and the intensities were quantitated with an LAS-4000 Image Analyzer (GE Healthcare). OC and SC indicate the open circular (relaxed) DNA and supercoiled DNA, respectively. Three independent experiments were performed, and the mean values are shown with the standard deviations. (D) tNASP titration experiments. The nucleosome assembly reactions were conducted with H3.1−H4 (lanes 1−5), H3.2−H4 (lanes 6−10), H3.3−H4 (lanes 11−15), and H3T−H4 (lanes 16−20), in the presence of H2A−H2B. The tNASP concentrations were 0 μM (lanes 1, 6, 11, and 16), 0.125 μM (lanes 2, 7, 12, and 17), 0.25 μM (lanes 3, 8, 13, and 18), 0.5 μM (lanes 4, 9, 14, and 19), and 1 μM (lanes 5, 10, 15, and 20). OC and SC indicate the open circular (relaxed) DNA and supercoiled DNA, respectively. (E) Graphic representation of the nucleosome-assembly activities of tNASP shown in panel D. The supercoiled DNA bands generated by tNASP-mediated nucleosome assembly are indicated by the arrows in panel D, and the intensities were quantitated with an LAS-4000 Image Analyzer (GE Healthcare). Three independent experiments were performed, and the mean values are shown with the standard deviations.

tNASP exhibited extremely weak activity for nucleosome assembly with the canonical H3.1 and H3.2, although it still promoted the nucleosome assembly with H3.3 (Figure 2C). A testis-specific histone H3 variant, H3T, was not efficiently incorporated into nucleosomes by either sNASP or tNASP (Figure 2C). Protein titration experiments confirmed that tNASP substantially promoted nucleosome assembly with H3.3, but it was very inefficient with H3.1, H3.2, and H3T (Figure 2D,E). These results suggested that H3.3 is a better substrate for the tNASP-mediated nucleosome assembly, as compared to H3.1 and H3.2.

The Ile89 Residue of H3.3 Is Required for the tNASP-mediated Nucleosome Assembly. In human histone H3.3, five amino acid residues, Ser31, Ala87, Ile89, Gly90, and Ser96, are not conserved in H3.1 (Figure 3A).[14] The H3.3 Ser31 residue is located in the unstructured N-terminal region, and the Ser96 residue is conserved in H3.2.[14] Therefore, to identify the H3.3 residues responsible for the tNASP-mediated nucleosome assembly, we focused on the H3.3-specific Ala87, Ile89, and Gly90 residues and prepared the H3.3 mutants, H3.3 A87S, H3.3 I89V, and H3.3 G90M, in which the Ala87, Ile89, and Gly90 residues were replaced by their corresponding H3.1 residues, Ser, Val, and Met, respectively (Figure 3B). We found that the tNASP-mediated nucleosome assembly activity was substantially reduced with H3.3 I89V, but not with H3.3 A87S (Figure 3C,D). The H3.3 G90M mutation moderately affected the tNASP-mediated nucleosome assembly activity (Figure 3C,D). Consistently, the H3.1 V89I mutation, in which the H3.1 Val89 residue was replaced by the corresponding H3.3 residue, Ile (Figure 3B), enhanced the tNASP-mediated

DOI: 10.1021/bi501307g
Biochemistry 2015, 54, 1171−1179

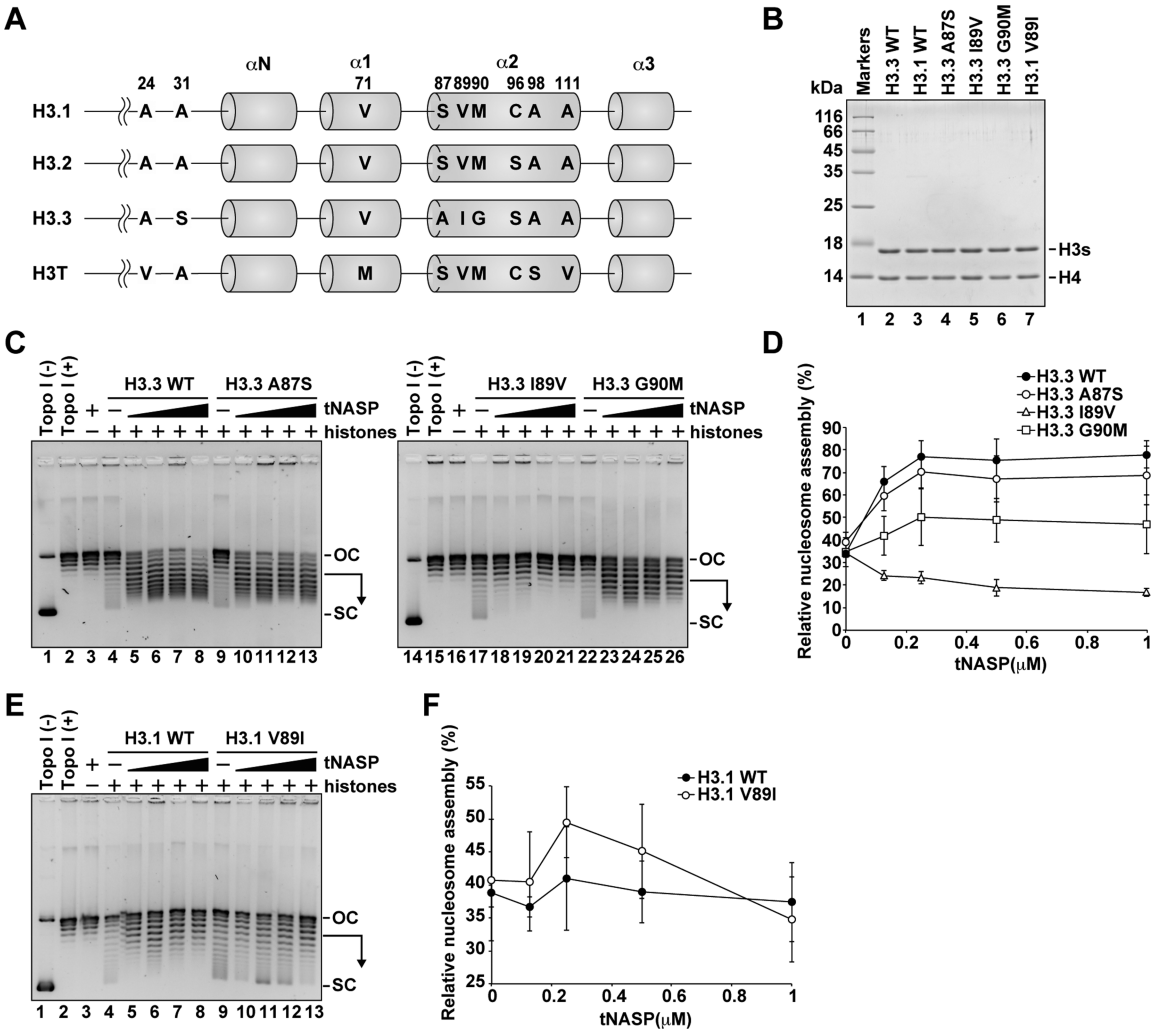

Figure 3. Mutational analyses of the H3.3 amino acid residues required for nucleosome assembly by tNASP. (A) Comparison of the amino acid sequences between H3.1, H3.2, H3.3, and H3T. Cylinders indicate the regions corresponding to helices in nucleosomes. (B) Purified H3.3 A87S, H3.3 I89V, H3.3 G90M, and H3.1 V89I mutants complexed with H4. Lanes 1, 2, and 3 indicate molecular mass markers, H3.3−H4 (wild type), and H3.1−H4 (wild type), respectively. H3.3 A87S−H4 (lane 4), H3.3 I89V−H4 (lane 5), H3.3 G90M−H4 (lane 6), and H3.1 V89I−H4 (lane 7) are shown. (C) tNASP-mediated supercoiling assay with H3.3 A87S, H3.3 I89V, and H3.3 G90M. Lanes 1 and 14 indicate the supercoiled DNA, and lanes 2 and 15 indicate the relaxed DNA. Lanes 3 and 16 indicate the negative control experiments without histones, in the presence of tNASP (1 μM). The wild type H3.3−H4 complex was used for positive control experiments (lanes 4−8). Lanes 9−13, 17−21, and 22−26 indicate the experiments with the H3.3 A87S−H4, H3.3 I89V−H4, and H3.3 G90M−H4 complexes, respectively. The protein concentrations of tNASP were 0.125 μM (lanes 5, 10, 18, and 23), 0.25 μM (lanes 6, 11, 19, and 24), 0.5 μM (lanes 7, 12, 20, and 25), and 1 μM (lanes 8, 13, 21, and 26). Lanes 4, 9, 17, and 22 indicate the experiments without tNASP, in the presence of histones. OC and SC indicate the open circular (relaxed) DNA and supercoiled DNA, respectively. (D) Graphic representation of the nucleosome-assembly activities of tNASP with the H3.3 mutants shown in panel C. The intensities of the supercoiled DNA bands generated by tNASP-mediated nucleosome assembly are indicated by the arrows in panel C and were quantitated with an LAS-4000 Image Analyzer (GE Healthcare). Three independent experiments were performed, and the mean values are shown with the standard deviations. (E) tNASP-mediated supercoiling assay with H3.1 V89I. The wild type H3.1−H4 complex was used for negative control experiments (lanes 4−8). Lanes 9−13 indicate the experiments with the H3.1 V89I mutant complexed with H4. The protein concentrations of tNASP were 0.125 μM (lanes 5 and 10), 0.25 μM (lanes 6 and 11), 0.5 μM (lanes 7 and 12), and 1 μM (lanes 8 and 13). Lanes 4 and 9 indicate the experiments without tNASP, in the presence of histones. OC and SC indicate the open circular (relaxed) DNA and supercoiled DNA, respectively. (F) Graphic representation of the nucleosome-assembly activities of tNASP with the H3.1 V89I mutant shown in panel E. The intensities of the supercoiled DNA bands generated by tNASP-mediated nucleosome assembly are indicated by the arrow in panel E and were quantitated with an LAS-4000 Image Analyzer (GE Healthcare). Three independent experiments were performed, and the mean values are shown with the standard deviations.

nucleosome assembly efficiency (Figure 3E), although it was somewhat inhibitory with a higher tNASP concentration (1 μM) for an unknown reason (Figure 3F). These results suggested that the Ile89 residue of H3.3 may be mainly responsible for efficient nucleosome assembly by tNASP.

H3.3-H4 Is Transferred to DNA by tNASP More Efficiently than H3.1−H4. We then tested whether tNASP binds to the H3.1−H4 complex used in the nucleosome assembly assay, by an electrophoretic mobility shift assay with a native polyacrylamide gel. When H3.1−H4 was incubated with tNASP, bands that migrated faster (lower) and slower (upper) than tNASP alone were detected (Figure 4A). These lower and upper bands were purified by preparative native polyacrylamide gel electrophoresis (Figure 4B). In the purified fractions, both

DOI: 10.1021/bi501307g
Biochemistry 2015, 54, 1171−1179

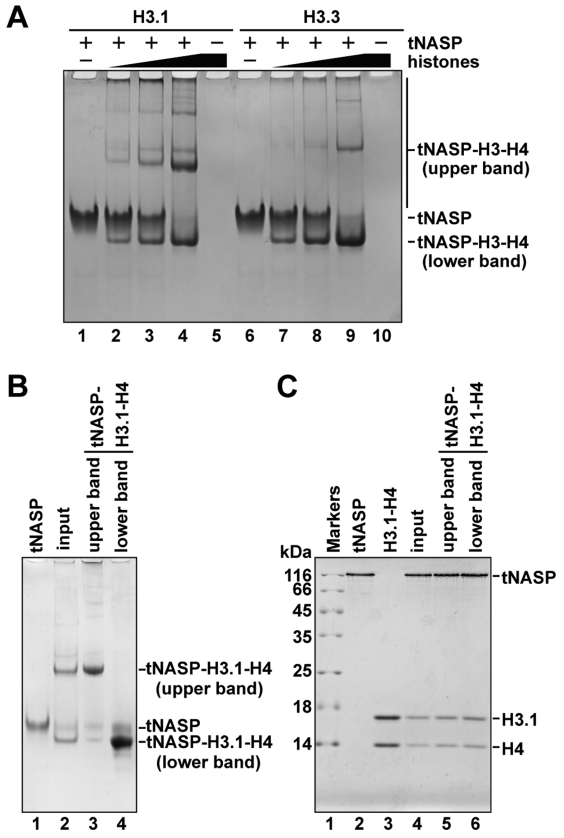

Figure 4. Histone binding activity of tNASP. (A) tNASP binds to H3.1−H4 and H3.3−H4. tNASP (3 μM) was incubated with H3.1−H4 (lanes 2−4) or H3.3−H4 (lanes 7−9). The resulting complexes were separated by 5% nondenaturing PAGE. The concentrations of H3.1−H4 or H3.3−H4 were 0 μM (lanes 1 and 6), 2.5 μM (lanes 2 and 7), 5 μM (lanes 3 and 8), and 10 μM (lanes 4, 5, 9, and 10). Lanes 5 and 10 indicate the control experiments without tNASP, in the presence of H3.1−H4 and H3.3−H4 (10 μM), respectively. The experiments with different protein concentrations were repeated at least twice, and consistent results were obtained. (B) Purification of the tNASP−H3.1−H4 complexes. The tNASP−H3.1−H4 complexes corresponding to the upper band (lane 3) and the lower band (lane 4) were purified by nondenaturing PAGE, using a Prep Cell apparatus. Lanes 1 and 2 indicate the tNASP and input tNASP−H3.1−H4 complexes, respectively. (C) SDS-PAGE analyses of the purified tNASP−H3.1−H4 complexes. Lanes 1, 2, and 3 indicate molecular mass markers, tNASP, and H3.1−H4, respectively. Lane 4 indicates the input sample. Lanes 5 and 6 indicate the proteins included in the complexes corresponding to the upper and lower bands, respectively.

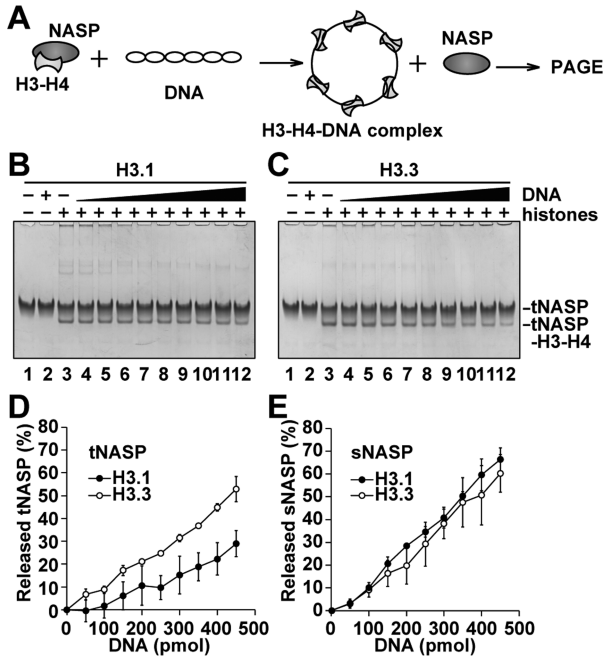

Figure 5. Histone deposition assay. (A) Schematic representation of the histone deposition assay. (B) tNASP-mediated H3.1−H4 deposition onto DNA. tNASP (6 μM) was incubated with the H3.1−H4 complex (6 μM) at 25 °C for 20 min, followed by an incubation at 25 °C for 60 min with the indicated amounts of supercoiled DNA. The complexes were then separated by 5% nondenaturing native polyacrylamide gel electrophoresis. The bands were visualized by Coomassie Brilliant Blue staining. The amounts of supercoiled DNA used in this assay were 0, 50, 100, 150, 200, 250, 300, 350, 400, and 450 pmol. (C) tNASP-mediated H3.3−H4 deposition onto DNA. tNASP (6 μM) was incubated with the H3.3−H4 complex (6 μM) at 25 °C for 20 min, followed by an incubation at 25 °C for 60 min with the indicated amounts of supercoiled DNA. The complexes were then separated by 5% nondenaturing native polyacrylamide gel electrophoresis. The bands were visualized by Coomassie Brilliant Blue staining. The amounts of supercoiled DNA used in this assay were 0, 50, 100, 150, 200, 250, 300, 350, 400, and 450 pmol. (D) Graphic representation of the tNASP-mediated H3.1−H4 (closed circles) and H3.3−H4 (open circles) deposition onto DNA. Representative images of the experiments are shown in panels B and C. The band intensities of the tNASP−H3−H4 complexes were quantitated, and the amounts of released tNASP were estimated relative to the input complex. Averages of three independent experiments were plotted with the standard deviations. (E) The sNASP-mediated deposition of H3.1−H4 (closed circles) and H3.3−H4 (open circles) onto DNA. sNASP (6 μM) was incubated with the H3.1−H4 or H3.3−H4 complex (10 μM) at 25 °C for 20 min, followed by an incubation at 25 °C for 60 min with the indicated amounts of supercoiled DNA. The complexes were then separated by 5% nondenaturing native polyacrylamide gel electrophoresis. The bands were visualized by Coomassie Brilliant Blue staining. The band intensities of sNASP were quantitated, and the amounts of released sNASP were estimated relative to the input sNASP. The amounts of supercoiled DNA used in this assay were 0, 50, 100, 150, 200, 250, 300, 350, 400, and 450 pmol. Averages of three independent experiments were plotted with the standard deviations.

complexes corresponding to the lower and upper bands contained tNASP, H3.1, and H4 (Figure 4C). These results indicated that the stable tNASP−H3.1−H4 complexes, which migrated differently on a native polyacrylamide gel, were actually formed. The stoichiometry of the tNASP−H3.1−H4 species in the lower band was quite similar to that of the upper band (Figure 4C), suggesting that the upper band may represent aggregates of the tNASP−H3.1−H4 complex detected in the lower band.

Our gel mobility shift assay revealed that tNASP also formed a complex with H3.3−H4, as well as H3.1−H4 (Figure 4A). During the nucleosome assembly process, the tNASP−H3−H4 complex deposits H3−H4 onto the DNA, and tNASP is released from the tNASP−H3−H4 complex. Therefore, the H3−H4 deposition rate can be monitored as the DNA-induced dissociation of the tNASP−H3−H4 complex (Figure 5A). We then evaluated the H3−H4 deposition activity of tNASP, by the competitive dissociation of the tNASP−H3.3−H4 complex by DNA. In this assay, the tNASP−H3.1−H4 and tNASP−H3.3−H4 complexes were formed using modified protein concentrations to eliminate the production of the upper bands. As shown in Figure 5B,C (lane 3), the initial amounts of the

DOI: 10.1021/bi501307g
Biochemistry 2015, 54, 1171−1179

tNASP−H3.1−H4 and tNASP−H3.3−H4 complexes were not significantly different under the assay conditions employed in these experiments. We then found that the tNASP−H3.3−H4 complex was dissociated more sensitively in the presence of DNA than the tNASP−H3.1−H4 complex (Figure 5B−D). This suggested that tNASP more efficiently deposited H3.3−H4 onto DNA than H3.1−H4. Interestingly, this H3.3−H4 preference in the histone deposition was not observed with sNASP, which deposited both H3.1−H4 and H3.3−H4 equally onto DNA (Figure 5E). Therefore, we concluded that tNASP preferentially promotes nucleosome assembly with H3.3, by its efficient H3.3−H4 deposition on the DNA.

DISCUSSION

Two spliced isoforms, tNASP and sNASP, were identified in humans.[43] Consistent with a previous observation, we detected the robust production of endogenous tNASP in testis; however, in the present study, we found that substantial amounts of tNASP are also produced in brain, heart, small intestine, kidney, liver, lung, skeletal muscle, stomach, spleen, and ovary (Figure 1D). These findings indicated that tNASP is not a testis-specific histone chaperone, and it ubiquitously functions in other tissues, as well as sNASP.[43]

Previous biochemical studies revealed that sNASP promotes nucleosome assembly with H3.1, H3.2, and H3.3, suggesting that it functions as a *bona fide* histone chaperone for H3−H4.[27,39] However, the biochemical analysis of tNASP has not been reported so far, since a purification method for tNASP has not been established. In the present study, we successfully purified human tNASP as a bacterially expressed recombinant protein, and performed biochemical analyses in vitro. We found that tNASP promotes nucleosome assembly with the replacement histone variant H3.3, while its activity is extremely low with canonical H3.1 and H3.2 (Figure 2). This result is in stark contrast to that with sNASP, which efficiently promotes nucleosome assembly with H3.1, H3.2, and H3.3.[27] These results suggest that tNASP may have a specific function with H3.3.

We previously found that the sNASP region containing amino acid residues 26−325 is required for efficient nucleosome assembly in vitro.[27] Interestingly, tNASP contains the 339 amino acid insertion after position 136, which is located in the middle of the 26−325 region of sNASP (Figure 1A). We found that tNASP does not efficiently deposit H3.1−H4 onto DNA, as compared to H3.3−H4 (Figure 5). The region with the extra 339 amino acids of tNASP somehow changes the histone H3−H4 deposition ability and may function in the specific chromatin incorporation of H3.3 isoforms.

Our mutational analysis revealed that the H3.3 Ile89 residue is important for the tNASP-mediated nucleosome assembly (Figure 3). The corresponding H3.1 residue is Val89. The side chain moiety of Ile is slightly different from the Val side chain, and has one additional methyl group. Such a small amino acid difference with one methyl group between H3T(Val111) and H3.1(Ala111) has been reported to significantly reduce the nucleosome stability.[45] Therefore, slight differences, such as the presence of one additional methyl group, in histones may have a drastic impact on the nucleosome formation and stability.

The Ala87, Ile89, and Gly90 residues of H3.3 are conserved in human H3.X and H3.Y, and the Ala87 and Gly90 residues are also conserved in human H3.5.[13] In the present study, we found that the Ile89 residue of H3.3 plays a crucial role in the tNASP-mediated nucleosome assembly. This suggests that H3.X and H3.Y may also be substrates for nucleosome assembly by tNASP, but H3.5 may not. Further studies are awaited to reveal how tNASP preferentially deposits H3.3−H4 onto DNA and promotes the H3.3 nucleosome assembly.

Massive nucleosome replacement by histone exchange occurs during spermatogenesis.[48,49] In mammals, meiotic sex-chromosome inactivation, in which the sex chromosomes are transcriptionally silenced, occurs during meiosis.[50−52] Intriguingly, de novo nucleosome assembly and the exclusive incorporation of H3.3 are promoted during the meiotic sex-chromosome inactivation process.[53] Further studies are needed to clarify the contributions of tNASP and sNASP in such histone exchange processes during mammalian spermatogenesis.

ASSOCIATED CONTENT

Supporting Information

Additional supplemental figure is available free of charge via the Internet at http://pubs.acs.org.

AUTHOR INFORMATION

Corresponding Author

*Tel. +81-3-5369-7315. Fax. +81-3-5367-2820. E-mail: kurumizaka@waseda.jp.

Funding

This work was supported in part by MEXT KAKENHI Grant Number 25116002 [to H.K.] and Grant Number 25131720 [to A.O.], JSPS KAKENHI Grant Number 25250023 [to H.K.], and the Platform for Drug Discovery, Informatics, and Structural Life Science from MEXT, Japan [to H.K.]. H.K. was also supported by the Waseda Research Institute for Science and Engineering, and Waseda University.

Notes

The authors declare no competing financial interest.

ACKNOWLEDGMENTS

We thank Ms. Sana Fujimaki (Waseda University) for her contribution in the initial stage of this project.

ABBREVIATIONS

NASP, nuclear autoantigenic sperm protein; PAGE, polyacrylamide gel electrophoresis; LB, lysogeny broth; IPTG, isopropyl β-D-thiogalactopyranoside; PMSF, phenylmethylsulfonyl fluoride; DTT, dithiothreitol; SDS, sodium dodecyl sulfate; EDTA, ethylenediaminetetraaceticacid

REFERENCES

(1) Wolffe, A. (1998) *Chromatin: Structure and Function*, 3rd ed., Academic Press, San Diego, California, USA.

(2) Arents, G., Burlingame, R. W., Wang, B. C., Love, W. E., and Moudrianakis, E. N. (1991) The nucleosomal core histone octamer at 3.1 Å resolution: a tripartite protein assembly and a left-handed superhelix. *Proc. Natl. Acad. Sci. U. S. A. 88*, 10148−10152.

(3) Zlatanova, J., Bishop, T. C., Victor, J.-M., Jackson, V., and van Holde, K. (2009) The Nucleosome Family: Dynamic and Growing. *Structure 17*, 160−171.

(4) Akey, C. W., and Luger, K. (2003) Histone chaperones and nucleosome assembly. *Curr. Opin. Struct. Biol. 13*, 6−14.

(5) Eitoku, M., Sato, L., Senda, T., and Horikoshi, M. (2007) Histone chaperones: 30 years from isolation to elucidation of the mechanisms of nucleosome assembly and disassembly. *Cell. Mol. Life Sci. 65*, 414−444.

DOI: 10.1021/bi501307g
Biochemistry 2015, 54, 1171−1179

(6) Andrews, A. J., Chen, X., Zevin, A., Stargell, L. A., and Luger, K. (2010) The histone chaperone Nap1 promotes nucleosome assembly by eliminating nonnucleosomal histone DNA interactions. *Mol. Cell 37*, 834−842.
(7) Avvakumov, N., Nourani, A., and Côté, J. (2011) Histone chaperones: modulators of chromatin marks. *Mol. Cell 41*, 502−514.
(8) Talbert, P. B., Ahmad, K., Almouzni, G., Ausió, J., Berger, F., Bhalla, P. L., Bonner, W. M., Cande, W. Z., Chadwick, B. P., Chan, S. W., Cross, G. A., Cui, L., Dimitrov, S. I., Doenecke, D., Eirin-López, J. M., Gorovsky, M. A., Hake, S. B., Hamkalo, B. A., Holec, S., Jacobsen, S. E., Kamieniarz, K., Khochbin, S., Ladurner, A. G., Landsman, D., Latham, J. A., Loppin, B., Malik, H. S., Marzluff, W. F., Pehrson, J. R., Postberg, J., Schneider, R., Singh, M. B., Smith, M. M., Thompson, E., Torres-Padilla, M. E., Tremethick, D. J., Turner, B. M., Waterborg, J. H., Wollmann, H., Yelagandula, R., Zhu, B., and Henikoff, S. (2012) A unified phylogeny-based nomenclature for histone variants. *Epigenetics Chromatin 5*, 7.
(9) Bönisch, C., and Hake, S. B. (2012) Histone H2A variants in nucleosomes and chromatin: more or less stable? *Nucleic Acids Res. 40*, 10719−10741.
(10) Filipescu, D., Szenker, E., and Almouzni, G. (2013) Developmental roles of histone H3 variants and their chaperones. *Trends Genet. 29*, 630−640.
(11) Talbert, P. B., and Henikoff, S. (2014) Environmental responses mediated by histone variants. *Trends Cell Biol. 24*, 642−650.
(12) Hake, S. B., and Allis, C. D. (2006) Histone H3 variants and their potential role in indexing mammalian genomes: the "H3 barcode hypothesis. *Proc. Natl. Acad. Sci. U. S. A. 103*, 6428−6435.
(13) Kurumizaka, H., Horikoshi, N., Tachiwana, H., and Kagawa, W. (2013) Current progress on structural studies of nucleosomes containing histone H3 variants. *Curr. Opin. Struct. Biol. 23*, 109−115.
(14) Hake, S. B., Garcia, B. A., Duncan, E. M., Kauer, M., Dellaire, G., Shabanowitz, J., Bazett-Jones, D. P., Allis, C. D., and Hunt, D. F. (2005) Expression patterns and post-translational modifications associated with mammalian histone H3 variants. *J. Biol. Chem. 281*, 559−568.
(15) Tachiwana, H., Osakabe, A., Shiga, T., Miya, Y., Kimura, H., Kagawa, W., and Kurumizaka, H. (2011) Structures of human nucleosomes containing major histone H3 variants. *Acta Crystallogr., Sect. D: Biol. Crystallogr. 67*, 578−583.
(16) Kaufman, P. D., Kobayashi, R., Kessler, N., and Stillman, B. (1995) The p150 and p60 subunits of chromatin assembly factor I: a molecular link between newly synthesized histones and DNA replication. *Cell 81*, 1105−1114.
(17) Gaillard, P. H., Martini, E. M., Kaufman, P. D., Stillman, B., Moustacchi, E., and Almouzni, G. (1996) Chromatin assembly coupled to DNA repair: a new role for chromatin assembly factor I. *Cell 86*, 887−896.
(18) Kamakaka, R. T., Bulger, M., Kaufman, P. D., Stillman, B., and Kadonaga, J. T. (1996) Postreplicative chromatin assembly by Drosophila and human chromatin assembly factor 1. *Mol. Cell. Biol. 16*, 810−817.
(19) Tagami, H., Ray-Gallet, D., Almouzni, G., and Nakatani, Y. (2004) Histone H3.1 and H3.3 complexes mediate nucleosome assembly pathways dependent or independent of DNA synthesis. *Cell 116*, 51−61.
(20) Ray-Gallet, D., Quivy, J. P., Scamps, C., Martini, E. M., Lipinski, M., and Almouzni, G. (2002) HIRA is critical for a nucleosome assembly pathway independent of DNA synthesis. *Mol. Cell 9*, 1091−1100.
(21) Lewis, P. W., Elsaesser, S. J., Noh, K. M., Stadler, S. C., and Allis, C. D. (2010) Daxx is an H3.3-specific histone chaperone and cooperates with ATRX in replication-independent chromatin assembly at telomeres. *Proc. Natl. Acad. Sci. U. S. A. 107*, 14075−14080.
(22) Drané, P., Ouararhni, K., Depaux, A., Shuaib, M., and Hamiche, A. (2010) The death-associated protein DAXX is a novel histone chaperone involved in the replication-independent deposition of H3.3. *Genes Dev. 24*, 1253−1265.
(23) Goldberg, A. D., Banaszynski, L. A., Noh, K. M., Lewis, P. W., Elsaesser, S. J., Stadler, S., Dewell, S., Law, M., Guo, X., Li, X., Wen, D., Chapgier, A., DeKelver, R. C., Miller, J. C., Lee, Y. L., Boydston, E. A., Holmes, M. C., Gregory, P. D., Greally, J. M., Rafii, S., Yang, C., Scambler, P. J., Garrick, D., Gibbons, R. J., Higgs, D. R., Cristea, I. M., Urnov, F. D., Zheng, D., and Allis, C. D. (2010) Distinct factors control histone variant H3.3 localization at specific genomic regions. *Cell 140*, 678−691.
(24) Dunleavy, E. M., Roche, D., Tagami, H., Lacoste, N., Ray-Gallet, D., Nakamura, Y., Daigo, Y., Nakatani, Y., and Almouzni-Pettinotti, G. (2009) HJURP is a cell-cycle-dependent maintenance and deposition factor of CENP-A at centromeres. *Cell 137*, 485−497.
(25) Foltz, D. R., Jansen, L. E., Bailey, A. O., Yates, J. R., 3rd, Bassett, E. A., Wood, S., Black, B. E., and Cleveland, D. W. (2009) Centromere-specific assembly of CENP-A nucleosomes is mediated by HJURP. *Cell 137*, 472−484.
(26) Tachiwana, H., Osakabe, A., Kimura, H., and Kurumizaka, H. (2008) Nucleosome formation with the testis-specific histone H3 variant, H3t, by human nucleosome assembly proteins in vitro. *Nucleic Acids Res. 36*, 2208−2218.
(27) Osakabe, A., Tachiwana, H., Matsunaga, T., Shiga, T., Nozawa, R. S., Obuse, C., and Kurumizaka, H. (2010) Nucleosome formation activity of human somatic nuclear autoantigenic sperm protein (sNASP). *J. Biol. Chem. 285*, 11913−11921.
(28) Shintomi, K., Iwabuchi, M., Saeki, H., Ura, K., Kishimoto, T., and Ohsumi, K. (2005) Nucleosome assembly protein-1 is a linker histone chaperone in Xenopus eggs. *Proc. Natl. Acad. Sci. U. S. A. 102*, 8210−8215.
(29) Alekseev, O. M., Widgren, E. E., Richardson, R. T., and O'Rand, M. G. (2005) Association of NASP with HSP90 in mouse spermatogenic cells: stimulation of ATPase activity and transport of linker histones into nuclei. *J. Biol. Chem. 280*, 2904−2911.
(30) Finn, R. M., Browne, K., Hodgson, K. C., and Ausió, J. (2008) sNASP, a histone H1-specific eukaryotic chaperone dimer that facilitates chromatin assembly. *Biophys. J. 95*, 1314−1325.
(31) Machida, S., Takaku, M., Ikura, M., Sun, J., Suzuki, H., Kobayashi, W., Kinomura, A., Osakabe, A., Tachiwana, H., Horikoshi, Y., Fukuto, A., Matsuda, R., Ura, K., Tashiro, S., Ikura, T., and Kurumizaka, H. (2014) Nap1 stimulates homologous recombination by RAD51 and RAD54 in higher-ordered chromatin containing histone H1. *Sci. Rep. 4*, 4863.
(32) Welch, J. E., Zimmerman, L. J., Joseph, D. R., and O'Rand, M. G. (1990) Characterization of a sperm-specific nuclear autoantigenic protein. I. Complete sequence and homology with the Xenopus protein, N1/N2. *Biol. Reprod. 43*, 559−568.
(33) Kleinschmidt, J. A., and Franke, W. W. (1982) Soluble acidic complexes containing histones H3 and H4 in nuclei of Xenopus laevis oocytes. *Cell 29*, 799−809.
(34) Kleinschmidt, J. A., Fortkamp, E., Krohne, G., Zentgraf, H., and Franke, W. W. (1985) Co-existence of two different types of soluble histone complexes in nuclei of Xenopus laevis oocytes. *J. Biol. Chem. 260*, 1166−1176.
(35) Kleinschmidt, J. A., Dingwall, C., Maier, G., and Franke, W. W. (1986) Molecular characterization of a karyophilic, histone-binding protein: cDNA cloning, amino acid sequence and expression of nuclear protein N1/N2 of Xenopus laevis. *EMBO J. 5*, 3547−3552.
(36) Ai, X., and Parthun, M. R. (2003) The nuclear Hat1p/Hat2p Complex: A molecular link between type B histone acetyltransferases and chromatin assembly. *Mol. Cell 14*, 195−205.
(37) Knapp, A. R., Wang, H., and Parthun, M. R. (2014) The yeast histone chaperone Hif1p functions with RNA in nucleosome assembly. *PLoS One 9*, e100299.
(38) Dunleavy, E. M., Pidoux, A. L., Monet, M., Bonilla, C., Richardson, W., Hamilton, G. L., Ekwall, K., McLaughlin, P. J., and Allshire, R. C. (2007) A NASP (N1/N2)-related protein, Sim3, binds CENP-A and is required for its deposition at fission yeast centromeres. *Mol. Cell 28*, 1029−1044.

DOI: 10.1021/bi501307g
Biochemistry 2015, 54, 1171−1179

(39) Wang, H., Walsh, S. T. R., and Parthun, M. R. (2008) Expanded binding specificity of the human histone chaperone NASP. *Nucleic Acids Res. 36*, 5763−5772.
(40) Cook, A. J. L., Gurard-Levin, Z. A., Vassias, I., and Almouzni, G. (2011) A specific function for the histone chaperone NASP to fine-tune a reservoir of soluble H3-H4 in the histone supply chain. *Mol. Cell 44*, 918−927.
(41) Wang, H., Ge, Z., Walsh, S. T. R., and Parthun, M. R. (2012) The human histone chaperone sNASP interacts with linker and core histones through distinct mechanisms. *Nucleic Acids Res. 40*, 660−669.
(42) Richardson, R. T., Alekseev, O. M., Grossman, G., Widgren, E. E., Thresher, R., Wagner, E. J., Sullivan, K. D., Marzluff, W. F., and O'Rand, M. G. (2006) Nuclear autoantigenic sperm protein (NASP), a linker histone chaperone that is required for cell proliferation. *J. Biol. Chem. 281*, 21526−21534.
(43) Richardson, R. T., Batova, I. N., Widgren, E. E., Zheng, L. X., Whitfield, M., Marzluff, W. F., and O'Rand, M. G. (2000) Characterization of the histone H1-binding protein, NASP, as a cell cycle-regulated somatic protein. *J. Biol. Chem. 275*, 30378−30386.
(44) Tanaka, Y., Tawaramoto-Sasanuma, M., Kawaguchi, S., Ohta, T., Yoda, K., Kurumizaka, H., and Yokoyama, S. (2004) Expression and purification of recombinant human histones. *Methods 33*, 3−11.
(45) Tachiwana, H., Kagawa, W., Osakabe, A., Kawaguchi, K., Shiga, T., Hayashi-Takanaka, Y., Kimura, H., and Kurumizaka, H. (2010) Structural basis of instability of the nucleosome containing a testis-specific histone variant, human H3T. *Proc. Natl. Acad. Sci. U. S. A. 107*, 10454−10459.
(46) Tachiwana, H., Kagawa, W., Shiga, T., Osakabe, A., Miya, Y., Saito, K., Hayashi-Takanaka, Y., Oda, Y., Sato, M., Park, S. Y., Kimura, H., and Kurumizaka, H. (2011) Crystal structure of the human centromeric nucleosome containing CENP-A. *Nature 476*, 232−235.
(47) Osakabe, A., Tachiwana, H., Takaku, M., Hori, T., Obuse, C., Kimura, H., Fukagawa, T., and Kurumizaka, H. (2013) Vertebrate Spt2 is a novel nucleolar histone chaperone that assists in ribosomal DNA transcription. *J. Cell Sci. 126*, 1323−1332.
(48) Rathke, C., Baarends, W. M., Awe, S., and Renkawitz-Pohl, R. (2014) Chromatin dynamics during spermiogenesis. *Biochem. Biophys. Acta 1839*, 155−168.
(49) Goudarzi, A., Shiota, H., Rousseaux, S., and Khochbin, S. (2014) Genome-scale acetylation-dependent histone eviction during spermatogenesis. *J. Mol. Biol. 426*, 3342−3349.
(50) Kierszenbaum, A. L., and Tres, L. L. (1974) Nucleolar and perichromosomal RNA synthesis during meiotic prophase in the mouse testis. *J. Cell Biol. 60*, 39−53.
(51) Turner, J. M., Mahadevaiah, S. K., Fernandez-Capetillo, O., Nussenzweig, A., Xu, X., Deng, C. X., and Burgoyne, P. S. (2005) Silencing of unsynapsed meiotic chromosomes in the mouse. *Nat. Genet. 37*, 41−47.
(52) Turner, J. M., Mahadevaiah, S. K., Ellis, P. J., Mitchell, M. J., and Burgoyne, P. S. (2006) Pachytene asynapsis drives meiotic sex chromosome inactivation and leads to substantial postmeiotic repression in spermatids. *Dev. Cell 10*, 521−529.
(53) van der Heijden, G. W., Derijck, A. A. H. A., Pósfai, E., Giele, M., Pelczar, P., Ramos, L., Wansink, D. G., van der Vlag, J., Peters, A. H. F. M., and de Boer, P. (2007) Chromosome-wide nucleosome replacement and H3.3 incorporation during mammalian meiotic sex chromosome inactivation. *Nat. Genet. 39*, 251−258.

DOI: 10.1021/bi501307g
Biochemistry 2015, 54, 1171−1179